2-15-1998

Effects of Cell Structure on the Reflection of Cholesteric Liquid Crystal Displays

Ming Xu
Kent State University - Kent Campus

Fudong Xu
Kent State University - Kent Campus

Deng-Ke Yang
Kent State University, dyang@kent.edu

Effects of cell structure on the reflection of cholesteric liquid crystal displays

Ming Xu, Fudong Xu, and Deng-Ke Yang[a)]
Liquid Crystal Institute and Chemical Physics Program, Kent State University, Kent, Ohio 44242

(Received 14 August 1997; accepted for publication 30 October 1997)

Cholesteric liquid crystal displays employ cells consisting of parallel glass plates which have indium-tin-oxide coating as the electrode and polyimide as the alignment layer. We have performed a systematic study of the reflections from the interfaces and the liquid crystal. We measured the reflection spectra using various incident light, various polarizations, and detection polarizations. Using the Berreman 4×4 method, we simulated the reflection spectra without fitting parameters; the results agreed well with the experimental results. © *1998 American Institute of Physics.* [S0021-8979(98)02104-5]

I. INTRODUCTION

Cholesteric liquid crystals are of great interest for reflective display applications and have been studied intensively recently.[1–7] When a cholesteric is sandwiched between two parallel glass plates, it exhibits three major textures: planar, focal conic, and homeotropic. When the liquid crystal is in the planar texture where the liquid crystal molecules have a helical structure with the helical axis perpendicular to the plates, the refractive index of the material exhibits a periodic structure along the cell normal, and the material Bragg reflects colored light. The reflected light is circularly polarized with the same handedness as the helical structure of the liquid crystal, and the reflection peak is centered at wavelength $\lambda = nP\cos\alpha$, where n is the average refractive index, P is the pitch of the liquid crystal, and α is the incident angle.[8] When the liquid crystal is in the focal conic texture where the helical axis is more or less parallel to the cell surface, it is optically scattering. When the liquid crystal is in the homeotropic texture where the helical structure is unwound, it is transparent. In reflective display applications, both the planar texture and the focal conic texture are stable at zero field while the homeotropic texture is achieved by application of an external field.[1–7] Cholesteric liquid crystals can also be used in eye-protection goggles operating between the reflective planar texture and transparent homeotropic texture.[9] Understanding the reflection of cholesteric liquid crystals is important for both basic science and applications. There are papers devoted to the optics of cholesteric liquid crystals in single domain and polydomain.[10–13] In the experimental studies, crossed polarizers were usually used in order to eliminate the complication caused by reflection from interfaces in cholesteric liquid crystal (Ch-LCD) cells. The results were in good agreement with the simulation using the Berreman 4×4 method with a few fitting parameters.

In a real Ch-LCD, the incident light is usually unpolarized and all reflected light is observed by human eyes. There are many layers in a Ch-LCD: glass plates, indium-tin-oxide (ITO) electrodes, alignment layers, and cholesteric liquid crystal. The reflections from the interfaces between the layers affect significantly the performance of the display. Therefore, it is important to understand the reflection caused by the various layers. In this article we report a systematic study of the reflections from the interfaces and the cholesteric liquid crystal in Ch-LCDs. Using the Berreman's 4×4 method, we can fit the experimental results very well.

II. SIMULATION

We used the Berreman 4×4 method to simulate the reflection spectra of CH-LCDs.[10,11] We chose the z axis perpendicular to the cell as shown in Fig. 1. The helical axis of the cholesteric liquid crystal is parallel to z. The dielectric tensor is given by

$$\vec{\vec{\epsilon}}(z)=\begin{bmatrix}\epsilon_{11} & \epsilon_{12} & 0\\ \epsilon_{21} & \epsilon_{22} & 0\\ 0 & 0 & \epsilon_{33}\end{bmatrix}. \tag{1}$$

In an isotropic medium such as the glass plate, $\epsilon_{11}=\epsilon_{22}=\epsilon_{33}=n^2$ and $\epsilon_{12}=\epsilon_{21}=0$, where n is the refractive index of the medium. In the cholesteric liquid crystal,

$$\epsilon_{11}=\tfrac{1}{2}(\epsilon_{\parallel}+\epsilon_{\perp})+\tfrac{1}{2}(\epsilon_{\parallel}-\epsilon_{\perp})\cos[(4\pi/P)z], \tag{2a}$$

$$\epsilon_{22}=\tfrac{1}{2}(\epsilon_{\parallel}+\epsilon_{\perp})-\tfrac{1}{2}(\epsilon_{\parallel}-\epsilon_{\perp})\cos[(4\pi/P)z], \tag{2b}$$

$$\epsilon_{33}=\epsilon_{\perp}, \tag{2c}$$

$$\epsilon_{12}=\epsilon_{21}=\tfrac{1}{2}(\epsilon_{\parallel}-\epsilon_{\perp})\sin[(4\pi/P)z], \tag{2d}$$

where $\epsilon_{\parallel}$ and $\epsilon_{\perp}$ are the dielectric constants measured parallel and perpendicular to the liquid crystal director, respectively.

For a light with wavelength λ and propagating in a direction making an angle α with the z axis, the wavevector outside the Ch cell (including the glass plate, ITO electrode, and polyimide alignment layer) is $k_0=(2\pi)/\lambda$ and its com-

a)Author to whom correspondence should be addressed; electronic mail: dyang@kentvm.kent.edu

ponent in the x direction is $k_x = k_0 \sin\alpha$. Note k_x is the same inside and outside of the Ch cell because there is no free charge and $\nabla \cdot \mathbf{D} = 0$. Because the dielectric tensor varies only in the z direction, the electric field and the magnetic field of the light have only two independent components each. The Berreman vector is defined as $\Psi = (E_x, E_y, H_x, H_y)^T$. From Maxwell's equations, the Berreman equation can be obtained.

$$\frac{\partial \Psi}{\partial z} = ik_0 \begin{bmatrix} 0 & 0 & 0 & \eta_0\left(\frac{k_x^2}{k_0^2}\frac{1}{\epsilon_{33}} - 1\right) \\ 0 & 0 & \eta_0 & 0 \\ \frac{\epsilon_{21}}{\eta_0} & \frac{1}{\eta_0}\left(\epsilon_{22} - \frac{k_x^2}{k_0^2}\right) & 0 & 0 \\ -\frac{\epsilon_{11}}{\eta_0} & -\frac{\epsilon_{12}}{\eta_0} & 0 & 0 \end{bmatrix} \Psi = ik_0 \vec{\vec{Q}}(z) \cdot \Psi. \tag{3}$$

$\vec{\vec{Q}}$ is called the Berreman matrix. $\eta_0 = \sqrt{\mu_0/\epsilon_0} = 377\ \Omega$ is the impedance of a vacuum. For a sufficiently small increment Δz in z, the approximate solution of Ψ is

$$\Psi(z + \Delta z) = e^{ik_0 \vec{\vec{Q}}(z)\Delta z} \cdot \Psi(z). \tag{4}$$

We divide the Ch cell into N slabs with the slabs labeled by j and thickness Δz_j. The Berreman vectors at the top and the bottom of the cell are related by the equation

$$\Psi_{\text{bottom}} = e^{ik_0 \vec{\vec{Q}}(z_N)\Delta z_N} \cdot e^{ik_0 \vec{\vec{Q}}(z_N - 1)\Delta z_{N-1}} \cdot \ldots \cdot e^{ik_0 \vec{\vec{Q}}(z_1)\Delta z_1} \cdot \Psi_{\text{top}} = \vec{\vec{F}} \cdot \Psi_{\text{top}}. \tag{5}$$

At the top of the cell, there is incident light and reflected light, and therefore $\Psi_{\text{top}} = \Psi_i + \Psi_r$. At the bottom of the cell, there is only the transmitted light, and $\Psi_{\text{bottom}} = \Psi_t$

$$\Psi_t = \vec{\vec{F}} \cdot (\Psi_i + \Psi_r). \tag{6}$$

Outside the Ch cell, the medium is a vacuum and the dielectric dielectric tensor is uniform, and the Berreman vector has only two independent components. For the reflected light which is propagating along the $-z$ direction,

$$\Psi_r(3) = H_{xr} = \frac{\cos\alpha}{\eta_0}\Psi_r(2) = \frac{\cos\alpha}{\eta_0}E_{yr},$$

$$\Psi_r(4) = H_{yr} = -\frac{1}{\eta_0\cos\alpha}\Psi_r(1) = -\frac{1}{\eta_0\cos\alpha}E_{xr}.$$

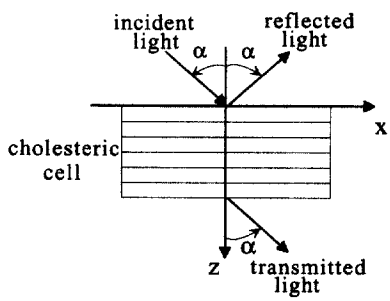

FIG. 1. The coordinate system used to describe the light propagation in the cholesteric cell in the simulation.

For transmitted light which is propagating along the z direction,

$$\Psi_t(3) = H_{xt} = -\frac{\cos\alpha}{\eta_0}\Psi_t(2) = -\frac{\cos\alpha}{\eta_0}E_{yt},$$

$$\Psi_t(4) = H_{yt} = \frac{1}{\eta_0\cos\alpha}\Psi_t(1) = \frac{1}{\eta_0\cos\alpha}E_{xt}.$$

Both Ψ_r and Ψ_t have two unknown variables. For a given incident light, Ψ_t and Ψ_r can be obtained by solving Eq. (6). In our simulation, the faster Berreman method, the Cayley–Hamilton theory, was used.[14]

III. EXPERIMENT AND RESULTS

In our experiment, a white light was generated by an arc lamp, and entered an Oriel monochromator with the resolution of 5 nm. The monochromatic light from the monochromator was collimated and incident on the cell at the angle of 22.5° with respect to the normal of the cell. The reflected light was detected by a photodiode. Reflection spectra were obtained by scanning the monochromator. Because of the 5 nm resolution of the monochromator, the reflectance was averaged over 5 nm in the simulation.

The cholesteric liquid crystal used was a mixture of 71.5 wt % nematic ZLI4330 and 28.5 wt % chiral dopant MLC-6247 (Merck). The dielectric anisotropy of the mixture was negative, and tended to be aligned perpendicular to the applied electric field. The material was filled into cells in a vacuum chamber. Before the optical measurement, an electric field was applied across the Ch cell to eliminate defects in the cell. The material was driven to the perfect planar texture, and remained in the perfect planar texture after the field was turned off.

The refractive indices of the cholesteric liquid crystal were unknown and was difficult to measure. We did not want to use the refractive indices as fitting parameters. In order to solve this problem, we made a racemic mixture of 71.5 wt % nematic ZLI4330 and 14.25 wt % right-handed chiral dopant MLC-6247 and 14.25 wt % left-handed chiral dopant MLC-

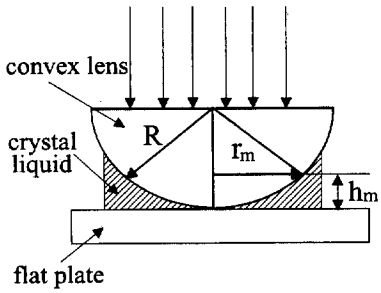

FIG. 2. The schematic diagram of the Newton's rings used to measure refractive indices and nematic liquid crystals.

6248. MLC-6247 and NLC-6248 are enantiomers and have the same refractive indices. The total concentration of the chiral dopants in the racemic mixture was the same as that in the cholesteric mixture, and the racemic mixture and the cholesteric mixture were expected to have the same refractive indices. We will further discuss the refractive indices of the mixture later. The racemic mixture was sandwiched between a flat glass plate and a convex lens having a spherical surface, as shown in Fig. 2. Both the flat glass plate and lens had homogeneous alignment layers, and the liquid crystal was aligned unidirectionally. Newton's rings were observed under an optical microscope illuminated by a sodium lamp. The radius of the spherical surface of the lens was known. In the measurement, one linear polarization was used. When light with polarization parallel to the liquid crystal director was used, the thickness h_m of the liquid crystal at the radius r_m of the mth dark ring is given by

$$2n_e h_m = (m + \tfrac{1}{2})\lambda.$$

On the other hand h_m is related to r_m by

$$h_m = R - \sqrt{R^2 - r_m^2} \approx \frac{1}{2R} r_m^2 \quad R \gg r_m.$$

Combining above two equations together, we get

$$r_m^2 = \frac{\lambda R}{n_e} m + \frac{\lambda R}{2n_e}.$$

When r_m^2 is plotted versus m, the slope is given by $(\lambda R)/(n_e)$. Therefore the refractive index can be obtained from the slope. We measured the extraordinary refractive index to be $n_e = 1.616$. When light with polarization perpendicular to the liquid crystal director was used, the ordinary refractive index was measured to be $n_0 = 1.494$. If crossed polarizers were used and the liquid crystal director made the angle 45° with the polarizers, then the birefringence can be measured directly.

We first measured the reflection spectrum of a 1.06 mm thick sodium lime glass plate which was obtained by etching off the ITO coating. Figure 3(a) shows the measured reflection spectra for the σ-polarization incident light (polarization direction perpendicular to the incident plane) and the π-polarization incident light (polarization direction in the incident plane). The simulated spectra are shown in Fig. 3(b), where the refractive index of 1.5 was used for the glass in the whole visible region. The interference between the light reflected from the top and bottom air–glass interfaces was not observed because the glass was thick and the resolution of the monochromator was limited.

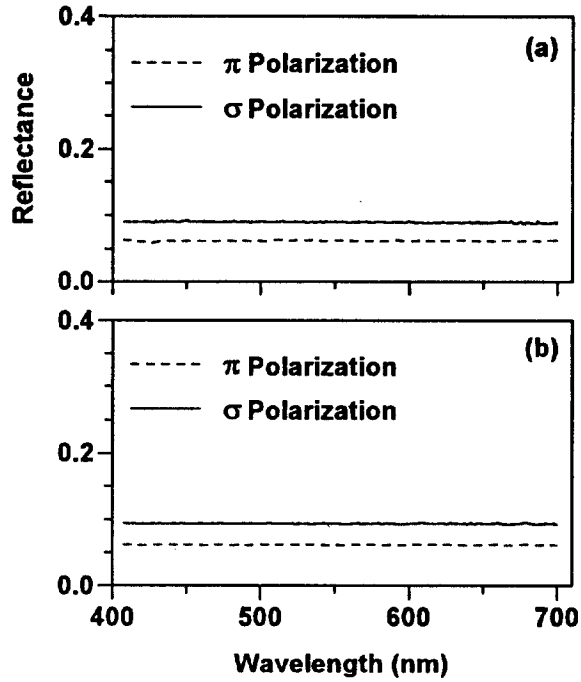

FIG. 3. Reflection spectra of a 1.06 mm thick sodium lime glass plate. (a) Experimentally measured spectra for the σ-polarization and π-polarization incident light. (b) Corresponding simulated spectra.

The measured reflection spectra of the glass with ITO coating are shown in Fig. 4(a) and the simulated reflection

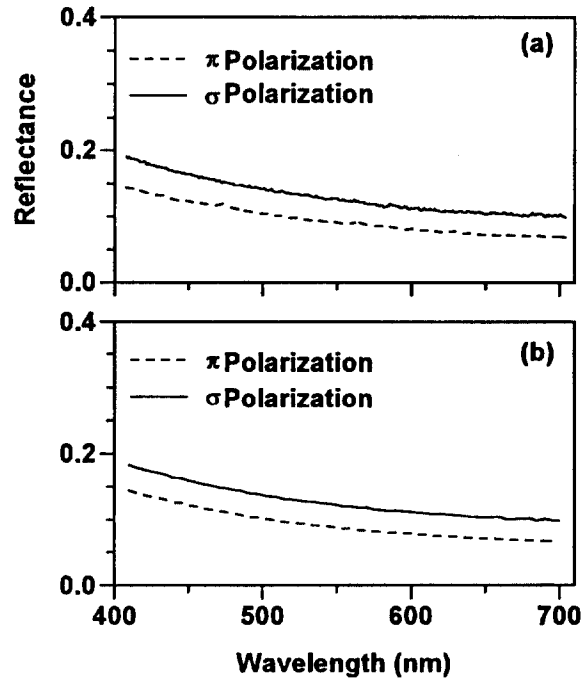

FIG. 4. Reflection spectra of the glass plate with ITO coating. (a) Experimentally measured spectra for the σ-polarization and π-polarization incident light. (b) Corresponding simulated spectra.

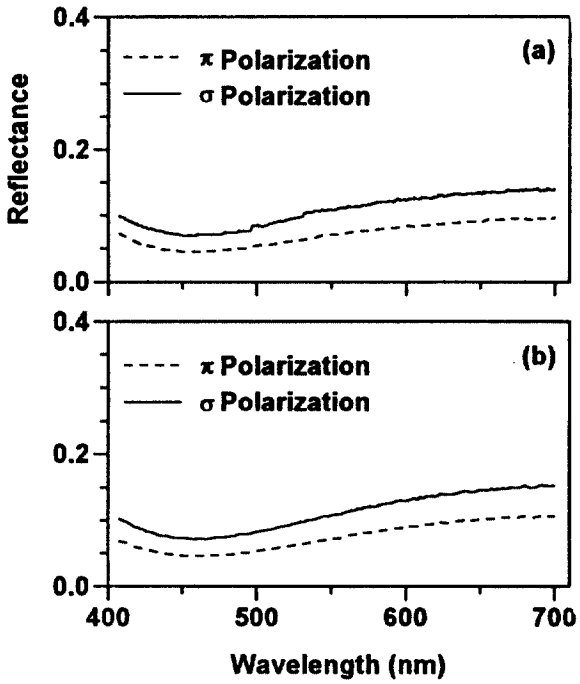

FIG. 5. Reflection spectra of the ITO coated glass plate with the polyimide alignment layer on top of the ITO. (a) Experimentally measured spectra for the σ-polarization and π-polarization incident light. (b) Corresponding simulated spectra.

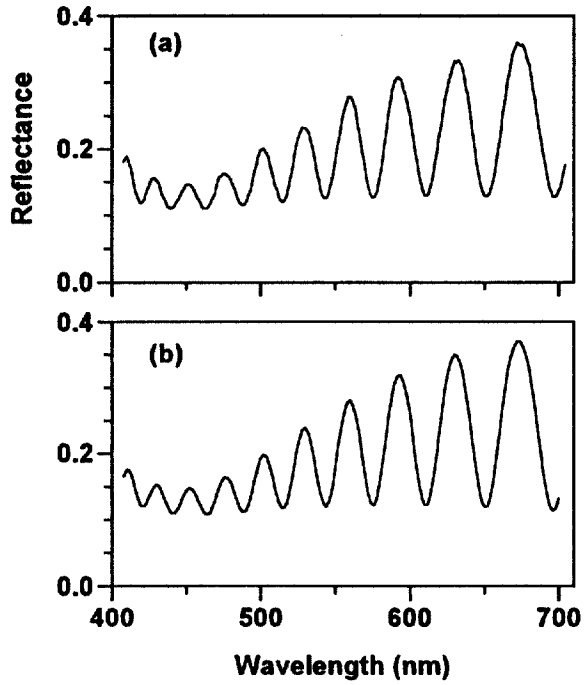

FIG. 6. Reflection spectra of an empty cell made of glass plates with the ITO and polyimide coating. (a) Experimentally measured spectrum for the σ-polarization. (b) Corresponding simulated spectrum.

spectra are shown in Fig. 4(b). The refractive index of the ITO coating depended on the wavelength and in the simulation the value $n(\lambda)=2.525-0.001271\lambda$ (the unit of λ was nm) was used.[15] The thickness of the ITO coating was 25 nm.[15] Very good agreement was achieved between the experimental and simulated spectra.

The Ch cells used had polyimide alignment layers on top of the ITO coating. The polyimide used was PI2555 (from DuPont). We measured the reflection spectra of the glass plate with the ITO coating and the polyimide alignment layer; the results are shown in Fig. 5(a). The thickness of the polyimide was 98 nm measured by a profilometer and the refractive index was 1.7 as specified by the manufacturer.[16] Using these parameters, the simulated reflection spectrum is shown in Fig. 5(b). In the short wavelength region, the polyimide had a refractive index between those of the ITO and air, and therefore acted as an antireflector and reduced the reflection.

An empty cell made of the glass with the ITO coating and polyimide alignment layer had the reflection spectrum shown in Fig. 6(a). In the measurement, σ polarization was used. The maxima and minima were caused by the interference between the reflected light from the two inner polyimide–air interfaces. In fabricating the cell, 5 μm glass fiber spacer was used. Empty (uncompressed) cells usually have cell gaps larger than the spacer. The simulated spectrum with a 5270 nm cell gap is shown in Fig. 6(b). One important point to note is how should be a cell gap measured. Cell gaps are usually measured in the following way. First, the reflection spectrum is measured, and the wavelengths of the minima (or maxima) of the interference are obtained. The wavelengths of the minima are given by $m\lambda_m=2h$, where m is an integer indicating the number of the minimum and h is the cell gap. $1/\lambda_m=1/(2h)m$. Then $1/\lambda_m$ is plotted versus m and the cell gap h is obtained from the slope of the line. Let us call this peak-wavelength method. This method is good if the glass of the cell does not have ITO coating and polymer alignment layer. If the glass has an ITO coating and a polymer coating, the cell gap obtained by the above method is no longer accurate. The accurate cell gap can be obtained by fitting the measured spectrum using the Berreman method. In order to illustrate the error in these two methods, we simulated the reflection spectra of a 5000 nm cell with and without the ITO coating and polyimide layer; the results are shown in Fig. 7. The maxima and minima of the cell with the

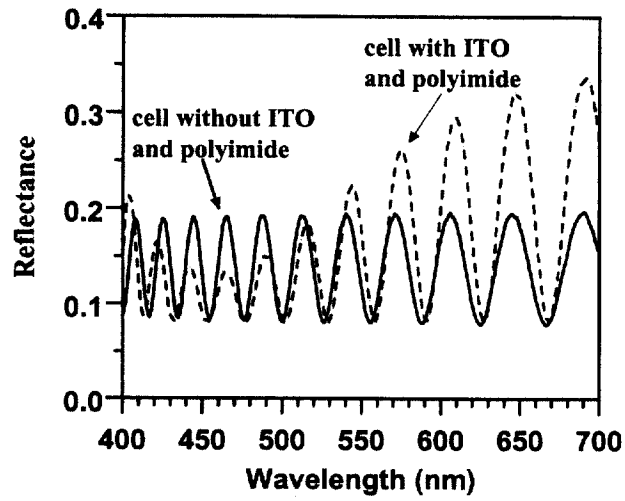

FIG. 7. Simulated spectra of empty cells made of glass plates with and without the ITO and polyimide coating for σ polarization.

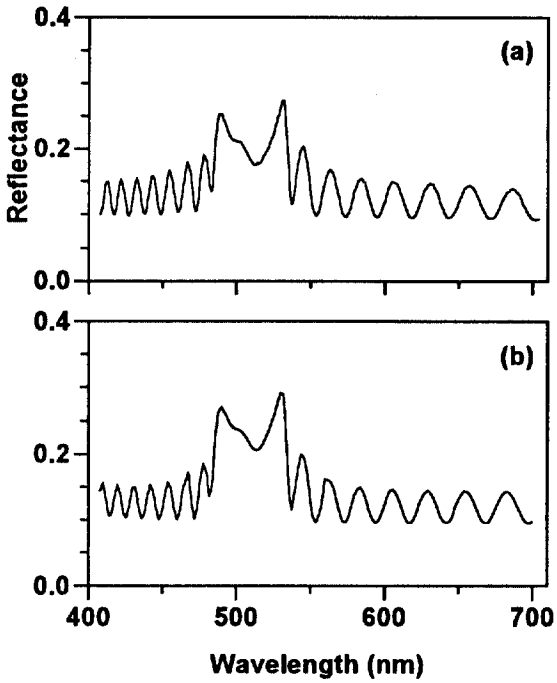

FIG. 8. Reflection spectra of the cholesteric cell for σ-polarization incident light and σ-polarization detection. The rubbing direction of the polyimide was perpendicular to the incident plane. (a) Experimentally measured spectrum. (b) Corresponding simulated spectrum with the pitch 338 nm and cell gap 5070 nm.

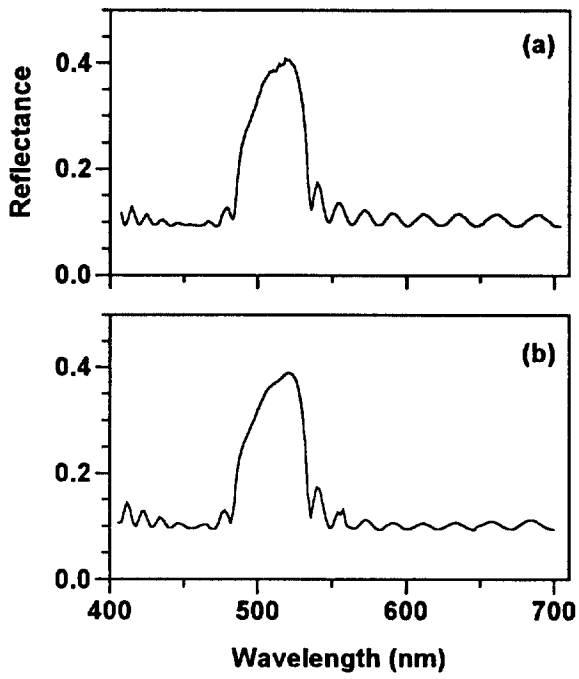

FIG. 9. Reflection spectra of the cholesteric cell for σ-polarization incident light and the σ-polarization detection. The the rubbing direction of the polyimide was in the incident plane. (a) Experimentally measured spectrum. (b) Corresponding simulated spectrum.

coatings are shifted by the coatings.[17] Then we calculate the cell gap using the peak-wavelength method. The cell gap of the cell without the ITO coating and polyimide was found to be 5003 nm (0.06% error), and the cell gap of the cell with the ITO coating and polyimide was found to be 4868 nm (2.6% error).

Finally, we studied the reflectivity of the cholesteric cell. The perfect planar texture was obtained by applying an external electric field as discussed in the sample preparation section. After the material was filled into the cell, the cell was compressed, and the cell gap was thinner than that of the empty cell. The pitch of the cholesteric liquid crystal was quantized to match the homogeneous boundary condition created by the polyimide alignment layer, and therefore $h/(0.5P)$ was an integer. The incident light had σ polarization and the reflected light with σ polarization was detected. When the polyimide rubbing direction was perpendicular to the incident plane, the measured and the simulated spectra are shown in Figs. 8(a) and 8(b), respectively. In the simulation, the measured refractive indices $n_e = 1.616$, $n_0 = 1.494$ were used. The unknown parameters were the pitch P and the cell gap h. The helical twisting power of MLC6247 was around 10 μm^{-1} and the mixture with 28.5% MLC6247 would have a pitch around 350 nm. By fitting the reflection spectrum and using the equation $h/(0.5P)$ = integer, we obtained $h = 5070.0$ nm and $P = 338$ nm $[h/(0.5P) = 30]$. The value of the pitch affects only the position of the reflection band but not the shape of the band. We used these parameters in the future simulation of the reflection spectra of the cholesteric liquid crystal under different polarization conditions. Figure 8(a) and Fig. 8(b) agree well. When the incident light was σ polarized and σ-polarized light was detected, but the cell was rotated 90° such that the polyimide rubbing direction was in the incident plane, the measured and simulated spectra are shown in Figs. 9(a) and 9(b), respectively. They agree well with each other, but differ significantly from Figs. 8(a) and 8(b). We looked into this difference. The reflection of a cholesteric cell was contributed by two reflections: the reflection from the cholesteric liquid crystal and the reflection from the interfaces. Both reflections have interference fringes. Under the conditions in Fig. 8, the two reflections were in phase and the amplitude of the interference fringes became larger. The dip in the reflection band was caused by the interference. Under conditions in Fig. 9, the two reflections were out of phase and the amplitude of the interference fringes became smaller, and therefore there was no dip in the reflection band. We ran simulation with different thickness of the polyimide layers, which only changed the phase of the reflection from the cholesteric liquid crystal, and found that the total reflection oscillated between those shown in Fig. 8 and Fig. 9.

When the reflection of the cholesteric cell was measured with crossed polarization (namely, σ-polarized incident light and π-polarized detection light), the measured and simulated spectra are shown in Figs. 10(a) and 10(b), and fit well. Now the reflections from the interfaces were eliminated by the crossed polarizers, and the background was zero. The measured reflection was solely from the cholesteric liquid crystal. From Fig. 5, we know that about 90% of the linearly polarized incident light reached the cholesteric liquid crystal. The incident light can be decomposed into left-handed polarized light and right-handed polarized light. The cell used was thick enough to reflect all the right-handed polarized light in the reflection band. The reflected right-handed polarized

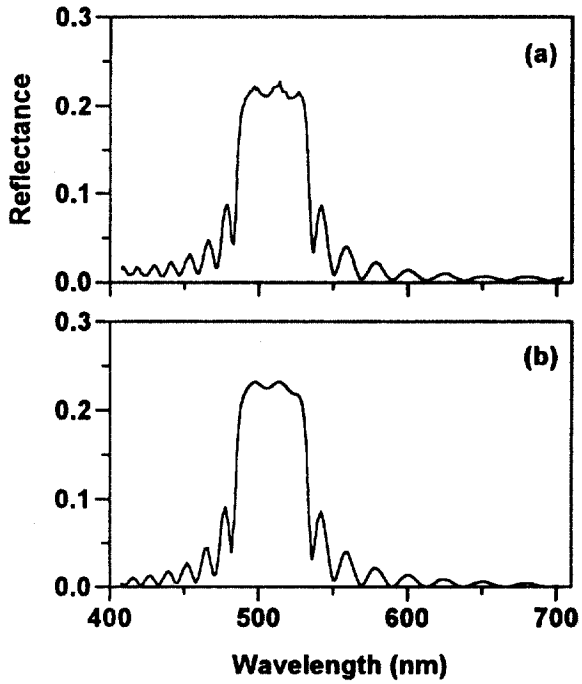

FIG. 10. Reflection spectra of the cholesteric cell for crossed polarization (σ-polarization incident light and π-polarization detection). (a) Experimentally measured spectrum. (b) Corresponding simulated spectrum.

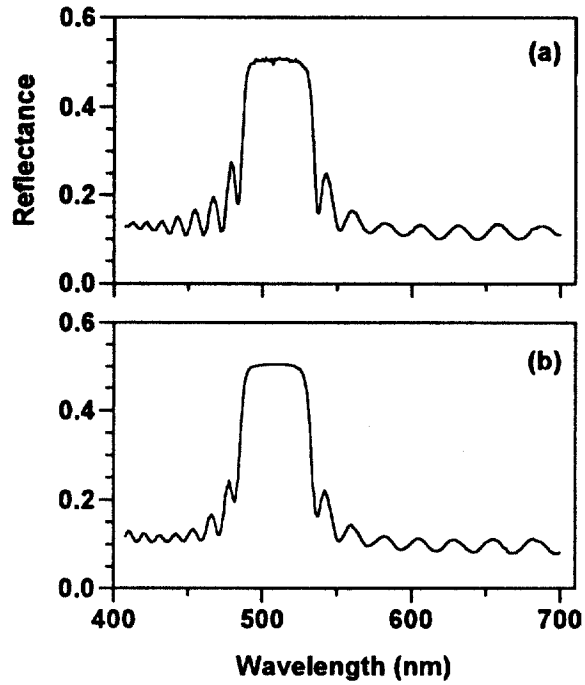

FIG. 11. Reflection spectra of the cholesteric cell without polarizers. (a) Experimentally measured spectrum. (b) Corresponding simulated spectrum.

light can be decomposed into σ and π components. The π component went through the analyzer: $0.9\times 1/2\times 1/2 = 0.225$. The reflection in the reflection band was 22.5%, as shown in Fig. 10.

We also studied the reflection of the cholesteric cell without polarizers. The incident light was unpolarized and all reflected light was measured. The measured and simulated spectra are shown in Figs. 11(a) and 11(b), and agree well. In this case, the simulated spectrum was obtained in the following way: using σ-polarized incident light and detecting all the reflected light, and using π-polarized incident light and detecting all the reflected light, then adding the intensity of the two reflected lights together. The reflection in the peak is slightly higher than 50% due to the interfaces. Under the same polarization condition, we measured and simulated the transmission spectra, and the results are shown in Figs. 12(a) and 12(b), respectively. When the reflection and transmission spectra are added, they equal 1, indicating our spectrometer and simulation program work properly.

In the simulation, we used the refractive indices of the racemic mixture for those of the cholesteric mixture. The refractive indices of a liquid crystal depend on the molecular polarizability of its components and the ordering of the molecules. The molecular polarizability of the left-handed and right-handed chiral molecules are the same. The molecular ordering of the racemic mixture and the cholesteric mixture is different. The racemic mixture exhibits the nematic phase and is usually uniaxial. The cholesteric mixture exhibits the cholesteric phase and is slightly biaxial.[18] In a cholesteric liquid crystal, molecules are parallel to each other in the plane perpendicular to the helical axis while the molecules are twisted with respect to each other in the helical axis direction. In principle, the local molecular arrangement is not identical in the nematic phase and the cholesteric phase. It was one of our motivations to investigate the local molecular arrangement in cholesteric liquid crystals and the effect of the cholesteric ordering on the refractive indices. Because the simulated spectra of the cholesteric cell using the refractive indices of the racemic mixture agree very well with the experimental results, we conclude that the biaxiality is insig-

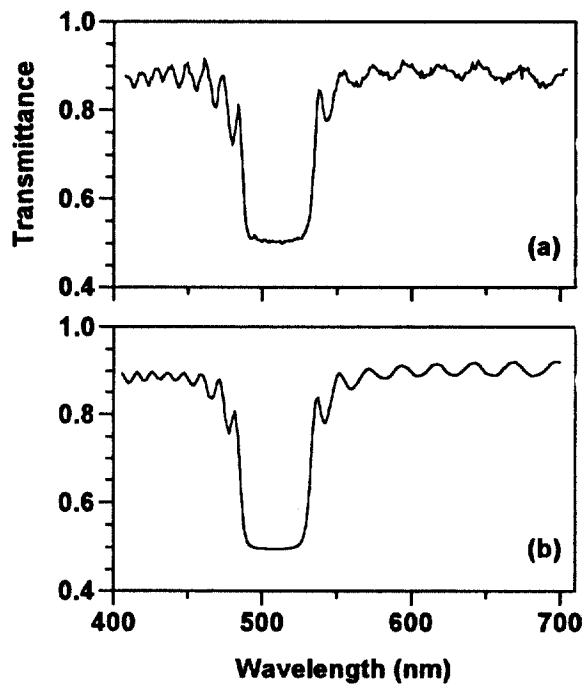

FIG. 12. Transmission spectra of the cholesteric cell without polarizers. (a) Experimentally measured spectrum. (b) Corresponding simulated spectrum.

nificantly small at the pitch length of 338 nm. The local molecular arrangement is practically the same in cholesteric and nematic phases.

IV. CONCLUSION

We have systematically studied the reflection of a cholesteric liquid crystal cell. The reflection spectra of interfaces and the cholesteric liquid crystal were measured one by one. The polarization dependence of the reflection was examined. We have also simulated the reflection spectra under various conditions. All the simulated spectra agree very well with the corresponding experimentally measured ones. The results will be very useful in understanding the reflection of cholesteric liquid crystals and in designing cholesteric displays.

ACKNOWLEDGMENTS

This research was supported in part by NSF under ALCOM-STC Grant No. DMR89-20147 and in part by an ARPA grant under Contract No. N61331-96-C-0042.

[1] W. Greubel, U. Wolff, and H. Kruger, Mol. Cryst. Liq. Cryst. **24**, (1973).
[2] G. A. Dir *et al.*, Proc. Soc. Inf. Disp. **13/2**, 106 (1972).
[3] D. K. Yang and J. W. Doane, SID Dig. Tech. Pap. 759 (1992).
[4] J. W. Doane, D. K. Yang, and Z. Yaniv, Proc. Jpn. Display '92, 73 (1992).
[5] D. K. Yang, J. L. West, L. C. Chien, and J. W. Doane, J. Appl. Phys. **76**, 1331 (1994).
[6] D. K. Yang, J. W. Doane, Z. Yaniv, and J. Glasser, Appl. Phys. Lett. **65**, 1905 (1994).
[7] D.-K. Yang and Z.-J. Lu, SID Intl. Symp. Digest, 351 (1995).
[8] For reviews on cholesteric liquid crystals, please see, S. Chandrasekhar, *Liquid Crystals* (Cambridge University Press, New York, Cambridge, 1992), pp. 213–297; P. G. de Gennes and P. Prost, *The Physics of Liquid Crystals* (Oxford University Press, New York, 1993), pp. 263–336.
[9] M. Xu and D.-K. Yang, Appl. Phys. Lett. **70**, 720 (1997).
[10] D. W. Berreman, J. Opt. Soc. Am. **62**, 502 (1972).
[11] D. W. Berreman and T. J. Scheffer, Mol. Cryst. Liq. Cryst. **11**, 395 (1970).
[12] I. Abdulhalim, L. Benguigui, and R. Weil, J. Phys. (France) **46**, 815 (1985).
[13] W. D. St. John, W. J. Fritz, Z. J. Lu, and D.-K. Yang, Phys. Rev. E **51**, 1191 (1995).
[14] W. L. Brogan, *Modern Control Theory*, 2nd ed. (Prentice-Hall, Englewood Cliffs, NJ, 1985).
[15] Private communication with J. Kelly. He measured the refractive index and thickness of the ITO using an ellipsometer.
[16] Data provided by Dupont Electronic Materials.
[17] K. H. Yang, J. Appl. Phys. **64**, 4780 (1988).
[18] Z. Yaniv, N. Vaz, G. Chidichimo, and J. W. Doane, Phys. Rev. Lett. **47**, 46 (1981).